Atmos. Chem. Phys. Discuss., 15, 23279–23315, 2015
www.atmos-chem-phys-discuss.net/15/23279/2015/
doi:10.5194/acpd-15-23279-2015

Atmospheric Chemistry and Physics
Discussions
Open Access

Retrieval of ammonia from ground-based FTIR solar spectra

E. Dammers[1], C. Vigouroux[2], M. Palm[3], E. Mahieu[4], T. Warneke[3], D. Smale[5], B. Langerock[2], B. Franco[4], M. Van Damme[1,6], M. Schaap[7], J. Notholt[3], and J. W. Erisman[1,8]

[1]Cluster Earth and Climate, Department of Earth Sciences, Vrije Universiteit Amsterdam, Amsterdam, the Netherlands
[2]Belgian Institute for Space Aeronomy, Brussels, Belgium
[3]Institut für Umweltphysik, University of Bremen, Bremen, Germany
[4]Institute of Astrophysics and Geophysics, University of Liege, Belgium
[5]National Institute of Water and Atmosphere, Lauder, New Zealand
[6]Spectroscopie de l'Atmosphère, Service de Chimie Quantique et Photophysique, Université Libre de Bruxelles, Brussels, Belgium
[7]TNO Built Environment and Geosciences, Department of Air Quality and Climate, Utrecht, the Netherlands
[8]Louis Bolk Institute, Driebergen, the Netherlands

Received: 1 June 2015 – Accepted: 9 August 2015 – Published: 28 August 2015

Correspondence to: E. Dammers (e.dammers@vu.nl)

Published by Copernicus Publications on behalf of the European Geosciences Union.

Abstract

We present a retrieval method for ammonia (NH_3) total columns from ground-based Fourier Transform InfraRed (FTIR) observations. Observations from Bremen (53.10° N, 8.85° E), Lauder (45.04° S, 169.68° E), Reunion (20.9° S, 55.50° E) and Jungfraujoch (46.55° N, 7.98° E) were used to illustrate the capabilities of the method. NH_3 mean total columns ranging three orders of magnitude were obtained with higher values at Bremen (mean of 13.47×10^{15} molecules cm^{-2}) to the lower values at Jungfraujoch (mean of 0.18×10^{15} molecules cm^{-2}). In conditions with high surface concentrations of ammonia, as in Bremen, it is possible to retrieve information on the vertical gradient as two layers can be discriminated. The retrieval there is most sensitive to ammonia in the planetary boundary layer, where the trace gas concentration is highest. For conditions with low concentrations only the total column can be retrieved. Combining the systematic and random errors we have a mean total error of 26 % for all spectra measured at Bremen (Number of spectra (N) = 554), 30 % for all spectra from Lauder (N = 2412), 25 % for spectra from Reunion (N = 1262) and 34 % for spectra measured at Jungfraujoch (N = 2702). The error is dominated by the systematic uncertainties in the spectroscopy parameters. Station specific seasonal cycles were found to be consistent with known seasonal cycles of the dominant ammonia sources in the station surroundings. The developed retrieval methodology from FTIR-instruments provides a new way to obtain highly time-resolved measurements of ammonia burdens. FTIR-NH_3 observations will be useful for understanding the dynamics of ammonia concentrations in the atmosphere and for satellite and model validation. It will also provide additional information to constrain the global ammonia budget.

1 Introduction

Nitrogen emissions in the form of ammonia (NH_3), which largely derive from agriculture, have been associated with acidification and eutrophication of soils and surface waters (Krupa, 2003; Vitousek et al., 1997), which may reduce biodiversity in vulnerable ecosystems (Bobbink et al., 1998, 2010). Ammonia also reacts with nitric acid and sulphuric acid to form ammonium salts, which account for a large fraction of particulate matter concentrations (Schaap et al., 2004). Particulate matter is major contributor to smog and is related to negative health impacts (Pope et al., 2009). Moreover ammonium salts play an important role in the radiance balance of the Earth, thus having an impact on climate change (Charlson et al., 1991; Erisman et al., 2007). Recently it was shown that reduced nitrogen also plays a role in the fixation of carbon dioxide (CO_2) (Reay et al., 2008). Human activities have increased the global emissions of reactive nitrogen (N_r) to the atmosphere (Holland et al., 1999). Current global N_r emissions have been estimated to be almost four times larger compared to pre-industrial levels (Fowler et al., 2013) with NH_3 emissions amounting to 49.3 Tg in 2008 (EDGAR-Emission Database for Global Atmospheric Research, 2011). Consequently this has led to large increases in atmospheric nitrogen deposition (Rodhe et al., 2002; Dentener et al., 2006). Biomass burning was found to account for 11 % of the global emission budget of NH_3 (Bouwman et al., 1997). While the agricultural emissions dominate in the Northern Hemisphere, biomass burning is one of the main sources of the NH_3 concentrations in the Southern Hemisphere.

Despite its central role in many environmental threats, little is known about the ammonia budget and its distribution across the globe. Uncertainties in global and regional emission rates are large with errors of more than 50 % (Erisman et al., 2007; Sutton et al., 2013). Ammonia concentrations have a large variability in time and space, a short lifetime in the order of hours, and the lack of globally distributed observations hamper our understanding. Surface observations are available but these are not homogenously distributed over the globe and most observation sites are located in the Northern Hemisphere. Most sites provide data with a poor temporal resolution e.g. many observation networks use passive samplers with a sampling time of 2 or 4 weeks (Thijsse et al., 1998; Puchalski et al., 2011) whereas emission and deposition dynamics affect concentrations on the scale of hours to days. Systems with higher sampling frequency such as the AMANDA, MARGA and (denuder) filter packs are available but the number of measurement networks using these instruments is limited as they are often costly to operate (Erisman et al., 2001; Thomas et al., 2009; Mount et al., 2002; Hansen et al., 2003). Moreover, measuring NH_3 is challenging and existing in-situ measurement techniques are often prone to sampling artefacts (von Bobrutzki et al., 2010). Recent advances in open path remote sensing techniques, like (mini-) DOAS systems and open path Quantum Cascaded Laser instruments show large potential to overcome part of these sampling issues (Volten et al., 2012; Miller et al.,2014), but are still in the development stage and not widely applied yet. Another aspect is the lack of vertical information, as most instruments only measure surface concentrations (Erisman et al., 1998, 2007; Van Damme et al., 2015a). Some recent airborne measurements have been made (Nowak et al., 2007, 2010; Leen et al., 2013) but only during dedicated campaigns with limited temporal and spatial coverage. In short, it is very difficult to obtain detailed knowledge on the global ammonia budget using currently available field observations.

Remote sensing products from atmospheric satellite sounders such as the Infrared Atmospheric Sounding Interferometer (IASI), the Tropospheric Emission Spectrometer (TES) and the Cross-track Infrared Sounder (CR-IS) (Van Damme et al., 2014a; Shephard et al., 2011) have become available and show good promise to improve NH_3 concentration monitoring (Van Damme et al., 2014b; Luo et al., 2015; Whitburn et al., 2015). However, these data sets are constrained by the overpass time of the satellite and the atmospheric conditions (cloud coverage, thermal contrast, etc.). Moreover, the uncertainties associated to the data are relatively large, which calls for a detailed evaluation of the data. A recent study (Van Damme et al., 2015a) showed a number of challenges related to the validation. First, reliable hourly in-situ data is sparse.

Second, when not using optimal estimation satellite product as is the case for the IASI-NH_3 retrieval, one has to assume a vertical profile to link surface concentrations to a column value. Third, the ground-based observations are often influenced by local sources, whereas the IASI satellite data are averaged observations over a circular footprint with at best a diameter of 12 km. Hence, a measurement methodology that would provide columnar and vertical profiles of ammonia concentrations at a high temporal resolution would be highly beneficial for evaluating the merits of the novel satellite products. Fourier Transform infrared spectrometry (FTIR) provides this methodology. Atmospheric sounders have a long history for validation of satellite products. FTIR observations are already commonly used for the validation of satellite products of among others, Carbon monoxide (CO), Methane (CH_4) and Nitrous Oxide (N_2O) (Kerzenmacher et al., 2012; Dils et al., 2006).

FTIR spectrometry is a well-established remote sensing technique for the observation of atmospheric trace gases (Rao and Weber, 1992). FTIR has so far been used to estimate ammonia emissions from fires by Paton-Walsh et al. (2005) but only on a campaign basis, not long-term monitoring. There are several monitoring stations with FTIR instruments operated on a regular basis, providing long-term time series for a suite of key tropospheric and stratospheric species, including Carbon Dioxide (CO_2), Carbon Monoxide (CO) and Ozone (O_3). So far nobody has systematically analysed the FTIR measurements for NH_3. We have developed a NH_3 retrieval strategies for four Network for detection of Atmospheric Composition Change (NDACC) FTIR stations, spanning very different concentration conditions (polluted and remote sites), in order to obtain time-series of NH_3 total columns and show its value for describing temporal variations.

First we present the measurement sites and the retrieval strategies in Sect. 2. We describe the characteristics of the retrieval in Sect. 3.1.1 and the uncertainty budget in Sect. 3.1.2. Section 3.2 constitutes of an interpretation of the results in combination with a comparison with existing datasets of CO total columns and temperature to distinguish between emission sources. We summarize the results in Sect. 4.

2 Measurement sites and retrieval strategies

2.1 Sites description

Ground-based FTIR instruments measure the solar absorption spectra under cloud-free conditions by using a Fourier Transform Spectrometer. These spectra can be analysed by using a line by line model (Pougatchev et al., 1995; Hase et al., 2004, 2006), which models the spectroscopic absorption lines by using known parameters from a spectroscopic database (e.g. HITRAN, Rothman et al., 2013) in combination with the radiative state of the atmosphere, and an optimal estimation inversion scheme (Rodgers, 2000). Information on vertical concentration profiles can be retrieved using the pressure broadening of the absorption lines. For the NDACC network the spectral region measured is the near- to mid-infrared domain (740 to 4250 $\mathrm{cm^{-1}}$, i.e. 13.5 to 2.4 µm) and a HgCdTe or InSb cooled detector (Zander et al., 2008) and a suite of optical filters are used to optimize the signal-to-noise ratio in the complementary spectral regions. Instruments in the network are routinely checked and characterized using laboratory measurements of HBr lines and the linefit software (Hase et al., 1999) to assess the instrument line shape, alignment and measurement noise levels. Four NDACC stations are used in our study, two in each hemisphere:

- The site of Bremen (53.10° N, 8.85° E) is especially suitable to measure variations in ammonia concentrations as the surrounding state, Lower Saxony, which is a region with intensive agricultural activities with high and temporal variable emissions (Dämmgen et al., 2005). In short, the ammonia total columns (molecules $\mathrm{cm^{-2}}$) at Bremen are expected to reach high values compared to background stations. The Universität Bremen operates a Bruker 125HR spectrometer and a solar tracker by Bruker GmbH, directly on the university campus.
- The Jungfraujoch station (46.55° N, 7.98° E) is a high altitude station (3580 m a.s.l.) located in Switzerland (Zander et al., 2008). There are no large emissions sources surrounding the station itself as it is mostly located in the free

troposphere. At Jungfraujoch, a Bruker 120HR instrument is in operation since the early 1990s. For the current study, specific for the Jungfraujoch site, we used a subset of spectra recorded during the 2004–2013 time period with apparent solar zenith angles (SZA) between 70 and 85° to increase the capability to retrieve the very low ammonia concentrations.

- The Lauder (45.04° S, 169.68° E) National Institute of Water and Atmospheric Research (NIWA) atmospheric research station in Central Otago, New Zealand at an altitude of 370 (m a.s.l.). Long-term operations started in 1991 with a Bruker 120M (Griffith et al., 2003). This instrument was replaced with a Bruker 120HR in October 2001. Ammonia emissions in the surrounding valley are mostly due to livestock grazing on the pastures and a by-product of seasonal fertilizer application. In recent years there has been an increase in cattle grazing and crop cultivation (EDGAR-Emission Database for Global Atmospheric Research, 2011).
- Reunion Island (20.9° S, 55.50° E) is located in the Indian Ocean to the east of Madagascar. The station is located at the University campus of St.-Denis on the north side of the island. Agricultural activities are mostly related to sugar cane production. The island is prone to some local biomass burning and wild fire events, which are known to emit ammonia. It is also very close to Madagascar, a region with frequent and intense biomass burning events, and it has been found using backward trajectory that the emissions in Madagascar can be transported to Reunion Island within one day (Vigouroux et al., 2009). The measurements used in this study are performed with a Bruker 120M spectrometer. Details on the measurements can be found in Senten et al. (2008) and Vigouroux et al. (2012).

These stations are expected to provide significant differences in variability and levels of ammonia, making them suitable to demonstrate the strength of our retrieval scheme for application across the whole network. A summary of the station descriptions is given in Table 1. CO columns were obtained from the NDACC database to be used for comparison in Sect. 3.

2.2 NH_3 retrieval strategies

The ammonia absorption lines from its υ_2 vibrational band can be observed in the 700–1350 cm^{-1} wavenumber range, which are also used in the retrieval of satellite products of ammonia (e.g. Clarisse et al., 2009; Van Damme et al., 2014a). In this spectral range the FTIR spectra can be measured using a potassium bromide (KBr) beam-splitter in combination with a mercury cadmium telluride (MCT) nitrogen cooled detector (Zander et al., 2008). The retrieval scheme of trace gas concentrations from FTIR spectra is built on the use of a set of spectral micro windows containing absorption lines of the targeted species, with minimum interference by other atmospheric species or solar lines. Two slightly different set of spectral micro-windows were used at the four stations, but they both use the same main NH_3 absorption lines. The target and interfering species are summarized in Table 2, with the profile retrieved species indicated in bold. To properly estimate ammonia, interfering species like O_3 and water vapour (H_2O) that overlap NH_3 lines in the υ_2 vibrational band have to be accounted for. Two micro windows were chosen that contain as little interfering species as possible. In both sets, the first micro window (MW1) covers the NH_3 absorption line at 930.75 cm^{-1}. At Bremen/Lauder, the choice was to use only isolated NH_3 absorption features to avoid possible problems due to line mixing, therefore the spectral window MW1 is only 1 cm^{-1} wide [930.32–931.32, MW1]. Figure 1 shows an example of a synthetic spectrum calculated to fit a observation that was measured with the 125HR in Bremen on the 19 April 2010 at 09:59 (UTC) (Solar Zenith Angle of 45°). The NH_3 concentrations on this day were slightly higher than average resulting in slightly stronger NH_3 absorption features in the spectra. The top two figures show the absorption contributions of the absorbing species in both micro windows. The bottom two panels show an enlarged version of the figure to distinguish the interfering species with smaller absorption features. At Reunion Island/Jungfraujoch, MW1 was extended [929.4–931.4, MW1] to cover another NH_3 line at 929.9 cm^{-1}. This improved the retrieval for Reunion Island because at this location the NH_3 concentration levels are much lower than at Bremen and the water vapour

Title Page
Abstract Introduction
Conclusions References
Tables Figures
◀| |▶
◀ ▶
Back Close
Full Screen / Esc
Printer-friendly Version
Interactive Discussion

concentrations are much higher. In this high humidity condition, the 930.75 cm^{-1} line is not isolated from H_2O, and it improved the retrieval to add the more isolated one at 929.9 cm^{-1} (see Fig. 2). The main interfering species in MW1 are CO_2, N_2O, and H_2O. Minor interfering species are SF_6 and CFC-12. The second window is spanning the NH_3 line at 967.35 cm^{-1}. Again, different widths are used for Bremen/Lauder [966.97–967.68, MW2] and Reunion Island/Jungfraujoch [962.7–970, MW2]. The very weak absorption signatures at Reunion Island and Jungfraujoch are close to the noise level and therefore the whole NH_3 absorption shape is retrieved (about 964–968 cm^{-1}, see Fig. 2) rather than a single line. The main interfering species in MW2 are O_3, CO_2 and H_2O for all sites. At Reunion Island HDO is also interfering in MW2 as well as the isotopologue $^{686}O_3$ (i.e. ^{16}O-^{18}O-^{16}O), which has been fitted in addition to the main $^{666}O_3$. At Jungfraujoch apart from CO_2, two O_3 isotopologues (the most abundant and $^{686}O_3$) and water vapour which are the main interferences, N_2O, CFC-12, SF_6 and HDO absorptions are also retrieved. Typical NH_3 absorptions are weak, on the order of a few tenths of a percent. The typical measurement noise (SNR) differs per spectra and site but ranges between ~ 250 at Lauder to ~ 450 at Bremen. Channelling was not an issue in any of the spectra and did not need to be fitted.

Except at Jungfraujoch where SFIT2 is used, the retrieval is performed using the more recent SFIT4.0.9.4 algorithm (Pougatchev et al., 1995; Hase et al., 2004, 2006). Both versions use a form of the optimal estimation method (Rodgers et al., 2000) to retrieve the volume mixing ratios and total columns of NH_3 and makes use of a-priori information (profile and covariance matrix). For Bremen, Lauder and Jungfraujoch the used NH_3 a-priori volume mixing ratios are based on balloon observations (Toon et al., 1999, NH_3 available in dataset but not reported). The shape of the balloon measurements profile was kept constant but extended and scaled to expected surface concentrations. The a-priori surface volume mixing ratio is estimated to be 10 ppb for Bremen (Dämmgen et al., 2005). Although the shape of NH_3 profiles do change through time, the largest share of NH_3 is expected to be in the mixing layer, which is represented by the lowest layers in the calculation (Van Damme et al., 2015a; Nowak et al., 2010). At Reunion Island, the a priori profile was taken from the MOZART model (Louisa Emmons, private communication). The a-priori profile peaks at a higher altitude (4–5 km) instead of the boundary layer as in Bremen, as NH_3 is expected to originate mainly from transport of biomass burning emissions at this location. At all stations, the a-priori profiles of the interfering species were taken from the Whole Atmosphere Community Climate Model (Chang et al., 2008).

At Bremen and Lauder, the a priori covariance matrices only have diagonal values corresponding to standard deviations of 100 % for all layers with no interlayer correlation, chosen in relation to the large range of possible concentrations and variations between layers. At Jungfraujoch and Reunion Island, we did not use the a priori covariance matrix as in optimal estimation but the Tikhonov type L_1 regularization (e.g. Sussmann et al., 2009) was adopted for the Jungfraujoch retrievals. After several tests, values of 50 and 250 were adopted for the alpha parameter and the signal to noise for inversion, respectively. A Tikhonov regularization with an alpha parameter value of 50 was also adopted for the Reunion retrievals. The signal to noise ratio is calculated for each spectra, the mean value being 365.

Daily temperature and pressure profiles for the meteorological variables were taken from NCEP (National Center for Environment Prediction). For the radiative transfer calculations the profiles were split into about 50 levels, depending slightly on the station, from ground up to 80 km (100 km in the case of Jungfraujoch and Reunion Island). The layers have a typical thickness of 500 m in the troposphere up to 2 km for the higher layers. For the line spectroscopy we use the HITRAN 2012 database (Rothman et al., 2013) in combination with a number of corrections for CO_2 (ATMOS, Brown et al.,1996) (except for Jungfraujoch for which the HITRAN lines are used) and sets of pseudo lines generated by G.C. Toon (NASA-JPL) to account for broad unresolved absorptions by heavy molecules (e.g. CFC-12, SF6).

Figure 3 shows an example of the fit in both micro windows for the same measured spectra as used in Fig. 1. The top two and bottom two panels show the calculated

(Green line) and measured spectrum (Blue line) and the residual of both micro windows. The simultaneous fits are good with a standard deviation of 0.15 % in both cases.

3 Results of the FTIR retrievals

3.1 Characteristics of the NH_3 retrievals

3.1.1 Vertical information

The retrieved vertical information differs from station to station. The top of Fig. 4 shows for the 4 stations the average NH_3 volume mixing ratios (VMR) for each of the retrieved layers (blue line) and the a priori profile that was used as input in the retrieval (green line). The bottom of Fig. 4 shows the averaging kernels for each of the 4 stations averaged over all available observations. As mentioned earlier most of the NH_3 at Bremen is in the lowest layers. In Fig. 4 this is also observed as the averaging kernel shows the most sensitivity in the lowest layers (red and green lines for the layers 0.03–0.5 and 0.5–1 km). The combination of the two spectral micro windows on average contain 1.9° of freedom for signal (DOFS) for the Bremen spectra, which means around two independent vertical layers can be retrieved. The two separate layers consist of a layer covering ground–1 km and one that covers 1–6 km height, which can be observed in Fig. 4. It must be taken into account however that the shown averaging kernels are a mean for all observations and thus the retrievable number of layers and combined layer depths vary from spectra to spectra. On average, the Lauder spectra have a DOFS of 1.4. There is only vertical information for multiple layers during periods with increased NH_3 total columns, which mostly occur during summer. Similar to Bremen averaging kernels peak near the surface. At Reunion Island only 1.0 DOFS is achieved, which means that only total columns can be retrieved. All the averaging kernels are peaking at the same altitude (about 5 km), which is also the peak of the a priori profile (Fig. 4). Similar to the Reunion spectra the Jungfraujoch spectra do not have vertical information with a DOF of 1.

3.1.2 Uncertainties budget

For the error analysis the posteriori error calculation included in the SFIT4 package is used. The error calculation is based on the error estimation approach by Rodgers (2000). It allows the calculation of the error by attributing errors to each of the parameters used in the retrieval. The error budget can be divided into three contributions, the error due to the forward model parameters, the measurement noise and the error due to the vertical resolution of the retrieval (smoothing error). The assumed uncertainties for the used parameters in the retrieval are listed in Table 3 for the parameters used in the calculation for Bremen, Lauder and Reunion. For Jungfraujoch, the error computation was performed using the perturbation method, the spectra of 2009 to 2011 and the Rodger formalism as explained e.g. in Franco et al. (2015). For Reunion Island, the covariance matrix used for the smoothing error has diagonal elements representing 150 % of variability from the a priori profile. To reflect the error in the NCEP temperature profiles we assume an uncertainty of about 2 K in the troposphere and a 5 K uncertainty in the stratosphere. For the uncertainty in the NH_3 line parameters we assume values as stated in the HITRAN 2012 database. We assume a conservative 20 % uncertainty for the intensity and 10 % for both the temperature and pressure broadening coefficients.

The results of the error calculation are listed in in Table 4. Combining the systematic and random errors we have a mean total error of 25.8 % for all the spectra measured at Bremen ($N = 554$), 30.2 % for the spectra from Lauder ($N = 2412$), 25.2 % for the Reunion spectra ($N = 1262$) and 34.23 % for the Jungfraujoch spectra ($N = 2702$). The errors are dominated by uncertainties in the spectroscopy. In detail, the random error sources amount to a mean error of 9.1 % for the Bremen spectra, which is mostly due to uncertainty in temperature, measurement noise and the zero level of the sensor (i.e. an instrument property). In the case of the systematic error, with a mean error of

23.5 %, the error is for the largest part due to the spectroscopy (i.e. line parameters) with smaller contributions of the temperature, zero level, phase and the smoothing error. The results are similar for the Lauder, Reunion and Jungfraujoch spectra with most of the uncertainty coming from the line parameters. Hence, the pressure and temperature broadening parameters of the ammonia absorption lines are critical for the NH_3 concentrations.

3.2 Time series

Figure 5 shows the NH_3 total columns retrieved from all available spectra from 2004–2013. Table 5 gives a summary of statistics of the retrieved NH_3 columns. Individual measurements at Bremen (blue) show high concentrations, especially in spring with an overall mean column total of 13.7×10^{15} molecules $NH_3\,cm^{-2}$ and a root mean square (RMS) of 20.22 indicating a large variability in the observations. The amplitude of the spring peaks vary throughout the years, with maxima in 2010 and 2013 reaching $\sim 93 \times 10^{15}$ and 85×10^{15} molecules $NH_3\,cm^{-2}$. The variability through the years is caused by changes in meteorology, emissions and timing of the measurements. Gaps in the data are due to days with overcast and instrument downtimes. The individual observed columns are sorted into monthly averages to analyse the seasonal variability and to understand the processes driving the NH_3 concentrations. This is shown in Fig. 6 together with monthly averages of surface temperature and CO total columns. NH_3 column total concentrations at Bremen (Blue line) have a seasonal cycle with highest levels during spring, the summer months and autumn. The maximum concentrations occur around April which is consistent with temporal emission patterns for manure application reported for this region (Friedrich and Reis, 2004; Martin et al., 2015; Paulot et al., 2014). The baseline variability with higher concentrations in summer can be explained by an increase in volatilization rates of NH_3, emitted from livestock housing, which is driven by animal activity and temperature (Gyldenkaerne et al., 2005). A comparison with CO is made to distinguish between agricultural and fire emissions sources.

A correlation between NH_3 and CO columns is not observed, which is consistent with agriculture as the dominant source of ammonia.

On average the measurements at Lauder (Fig. 5, red line, top panel) yield a column total of 4.17×10^{15} molecules NH_3 cm^{-2}. These levels are about 1/3 of the concentrations measured at Bremen (blue, top panel). Spectra from Lauder are available for most days in the retrieved time series, which makes it easier to discern peaks and variability. Distinctive peaks are only visible in the summers. Maxima during spring times are not often observed. The peak values are similar in between years, with maxima typically around 30×10^{15} molecules NH_3 cm^{-2}. As for Bremen the RMS of 5.95 reflects a large variability in the observations between individual retrievals. The average error is 1.34×10^{15} which is around a quarter of the mean. Figure 6 shows the seasonal cycle of Lauder (red line, top left panel). The seasonal variation of NH_3 coincides with that of the atmospheric temperature (red line, bottom right panel) and with the livestock emissions in the surrounding region, which are strongly correlated with temperature.

The bottom panel of Fig. 5 shows the observations from Reunion (green symbols, bottom panel). The mean column total observed at Reunion is 0.82×10^{15} molecules NH_3 cm^{-2}. The concentrations are low during most of the year. However, peaks reaching densities of $\sim 6 \times 10^{15}$ molecules NH_3 cm^{-2} can be observed during the end of each year. The peaks in September–November coincide with the dry season indicating that emissions are mostly due to biomass burning and large fire events (Vigouroux et al., 2012). This is supported by the increased CO concentrations, which are also observed in October and November (see, bottom left panel, Fig. 6). NH_3 surface concentration measurements are not available for this region but a recent paper by Van Damme et al. (2015b), which uses IASI-NH_3 observations, shows similar seasonal cycles for the south eastern parts of Africa (Madagascar). Temperature is almost constant throughout the year and not a major factor in the seasonality of Reunion.

Observations from Jungfraujoch have the lowest mean concentration of all four stations (Fig. 5, orange line), with a mean of 0.18×10^{15} molecules NH_3 cm^{-2}. The low concentrations at Jungfraujoch are expected, as the station is located in the free troposphere high above the surrounding valleys. Transport of NH_3 from the valleys only occurs sporadically during days with intense vertical mixing. This was also observed in an earlier study of CO concentrations (Barret et al., 2003). The Jungfraujoch observations show almost no seasonal effects with only a minimal increase during the summer months. The low concentrations measured at Jungfraujoch support our assumption on the vertical distribution of the ammonia concentrations with low values in the troposphere that were used in our a-priori.

4 Conclusions and perspectives

In this study we presented a new method to retrieve ammonia total columns from ground-based FTIR solar spectra. Observations from four complementary stations were used to illustrate the capabilities of the retrieval method. NH_3 total columns ranging three orders of magnitude were obtained with high abundances at Bremen (mean of 13.47×10^{15} molecules cm^{-2}) to low columns at Jungfraujoch (mean of 0.18×10^{15} molecules cm^{-2}). The very low levels obtained at the Jungfraujoch demonstrate the sensitivity of the retrieval method we developed. A separate error calculation shows random errors in the order of 10 % and systematic errors of 25 % for individual observations. The errors are dominated by uncertainties in spectroscopy, atmospheric temperature and deviations in instrumental parameters. For conditions with high surface concentrations of ammonia, as in Bremen, it is possible to retrieve information on the vertical gradient as two layers can be discriminated. At Bremen, the retrieval there is most sensitive to ammonia in the planetary boundary layer, where most of the ammonia is expected. For conditions with lower concentrations only the total columns can be retrieved. Station specific seasonal cycles were found to be consistent with known seasonal cycles of the dominant ammonia sources in the station surroundings. For example, highest levels in Bremen were observed during spring time when manure is applied to the fields with column total concentrations reaching up to 93×10^{15} molecules cm^{-2}.

Remote sensing techniques avoid sampling artefacts common to other techniques such as filter packs (Puchalski et al., 2011; von Bobrutzki et al., 2010). For in-situ observations open path remote sensing techniques, e.g. DOAS and QCL instruments, are starting to be used (Volten et al., 2010; Miller et al., 2014). The FTIR-NH_3 observations would be an excellent addition to these approaches as it provides the NH_3 total column and profiles, including vertical information for sites sampling high ammonia levels. With a mean error of ~ 25 % for all observations in high ammonia source areas the accuracy of the FTIR retrievals is comparable to that reported for satellite products (TES, IASI, CrIS). Compared to the in-situ open path remote sensing methods the FTIR method has a higher uncertainty, but this is a trade-off for the ability to retrieve vertical information. To improve the accuracy of the FTIR-NH_3 retrieval a reassessment of the spectral line parameters is necessary.

Observations from existing networks commonly represent daily or even monthly averaged concentration values, which severely complicates any attempt to validate satellite observations. The novel FTIR-NH_3 observations enable a direct validation of satellite products. As the FTIR-NH3 product provides averaging kernels a direct comparison can be made with optimal estimation satellite retrievals while taking account of the a-priori information and vertical sensitivity of both instruments (Rogers and Connor, 2003). A dedicated field campaign was executed at the Cabauw Experimental Site for Atmospheric Remote Sensing (CESAR) in the Netherlands (spring and summer 2014) to validate the IASI- NH_3 using a range of instruments including mini-DOAS instruments and a Bruker IFS-66 instrument (Dammers et al. in prep).

The uncertainty in the emission distributions hampers the performance and prediction capabilities of air quality and climate models (Heald et al., 2012). Emissions are usually based on nationally reported yearly emission inventories (Pouliot et al., 2012) and gridded by distributing the emissions following animal numbers and agricultural land use (Bouwman et al., 2002; Keunen et al., 2011). To improve on static emission time profiles, a new direction is to include the impact of meteorological variability of ammonia emissions in modelling systems (Sutton et al., 2013). Recently, such an improvement was shown to greatly enhance the performance of air quality models (Skjoth et al., 2011). Similar to satellite observations, FTIR total columns in combination with surface observations could provide the means to evaluate the emission modelling through comparing trends and concentration anomalies within and between years. For this purpose continuous time series are necessary. Due to the lack of continuous data (i.e. more than one observation per hour) we could not derive a typical diurnal cycle in this study, whereas this would be highly useful for model evaluation. Improved knowledge on the diurnal cycles may also greatly help to interpret model evaluation results against satellite data as they provide snapshots, e.g. daily IASI's observations at 9.30. Also, the model-measurement comparison would be less sensitive to modelling errors in the turbulent vertical exchange as the ammonia is integrated over vertical.

The developed retrieval methodology from FTIR-instruments provides a new way to obtain vertically and temporally resolved measurements on ammonia concentrations. FTIR-NH_3 observations may prove very valuable for satellite and model validation and may provide a complementary source of information to constrain the global ammonia budget.

Acknowledgements. This work is part of the research programme GO/12-36, which is financed by the Netherlands Organisation for Scientific Research (NWO). Acknowledgements are addressed to the Université de La Réunion and CNRS (LACy-UMR8105 and UMS3365) for their strong support of the OPAR station (Observatoire de Physique de l'Atmosphère de la Réunion) and the OSU-R (Observatoire des Sciences de l'Univers de la Réunion) activities. The authors gratefully acknowledge C. Hermans and F. Scolas from BIRA-IASB, and J.-M. Metzger from Université de La Réunion, for the Reunion Island measurements. We are also grateful to Louisa Emmons (NCAR) who provided NH_3 profiles from the MOZART model used as a priori in the Reunion Island retrievals. The University of Liège contribution to the present work has mainly been supported by the A3C project (PRODEX Program of the Belgian Science Policy Office, BELSPO, Brussels). Additional support was provided by MeteoSwiss (Global Atmospheric Watch), the Fédération Wallonie–Bruxelles and the F.R.S. – FNRS. We thank the International Foundation High Altitude Research Stations Jungfraujoch and Gornergrat (HFSJG, Bern). E. Mahieu is Research Associate with F.R.S. – FNRS. The Lauder NIWA FTIR program is funded through the New Zealand Government's core research grant framework. We are grateful to the many colleagues who have contributed to FTIR data acquisition at the various sites.

References

Barret, B., De Mazière, M., and Mahieu, E.: Ground-based FTIR measurements of CO from the Jungfraujoch: characterisation and comparison with in situ surface and MOPITT data, Atmos. Chem. Phys., 3, 2217–2223, doi:10.5194/acp-3-2217-2003, 2003.

Bobbink, R., Hornung, M., and Roelofs, J. G.: The effects of air-borne nitrogen pollutants on species diversity in natural and semi-natural European vegetation, J. Ecol., 86, 717–738, 1998.

Bobbink, R., Hicks, K., Galloway, J., Spranger, T., Alkemade, R., Ashmore, M., Bustamante, M., Cinderby, S., Davidson, E., Dentener, F., Emmett, B., Erisman, J. W., Fenn, M., Gilliam, F., Nordin, A., Pardo, L., De Vries, W.: Global assessment of nitrogen deposition effects on terrestrial plant diversity: a synthesis, Ecol. Appl., 20, 30–59, 2010.

Bouwman, A. F., Lee, D. S., Asman, W. A. H., Dentener, F. J., Van Der Hoek, K. W., and Olivier, J. G. J.: A global high-resolution emission inventory for ammonia, Global Biogeochem. Cy., 11, 561–587, 1997.

Bouwman, A. F., Boumans, L. J. M., and Batjes, N. H.: Estimation of global NH_3 volatilization loss from synthetic fertilizers and animal manure applied to arable lands and grasslands, Global Biogeochem. Cy., 16, 8-1–8-14, doi:10.1029/2000GB001389, 2002.

Brown, L. R., Gunson, M. R., Toth, R. A., Irion, F. W., Rinsland, C. P., and Goldman, A.: 1995 Atmospheric Trace Molecule Spectroscopy (ATMOS) linelist, Appl. Optics, 35, 2828–2848, 1996.

Chang, L., Palo, S., Hagan, M., Richter, J., Garcia, R., Riggin, D., and Fritts, D.: Structure of the migrating diurnal tide in the Whole Atmosphere Community Climate Model (WACCM), Adv. Space Res., 41, 1398–1407, doi:10.1016/j.asr.2007.03.035, 2008.

Charlson, R. J., Langner, J., Rodhe, H., Leovy, C. B., and Warren, S. G.: Perturbation of the Northern-Hemisphere radiative balance by backscattering from anthropogenic sulfate 15 aerosols, Tellus A, 43, 152–163, 1991.

Dämmgen, U. and Erisman, J. W.: Emission, Transmission, Deposition and Environmental Effects of Ammonia from Agricultural Sources, edited by: Kuczynski, T., Dämmgen, U., and

Webb, J., Emissions from European Agriculture, Wageningen Academic Publishers, Wageningen, 97–112, 2005.

Dentener, F., Drevet, J., Lamarque, J. F., Bey, I., Eickhout, B., Fiore, A. M., Hauglustaine, D., Horowitz, L. W., Krol, M., Kulshrestha, U. C., Lawrence, M., Galy-Lacaux, C., Rast, S., Shindell, D., Stevenson, D., Van Noije, T., Atherton, C., Bell, N., Bergman, D., Butler, T., Cofala, J., Collins, B., Doherty, R., Ellingsen, K., Galloway, J., Gauss, M., Montanaro, V., Müller, J. F., Pitari, G., Rodriguez, J., Sanderson, M., Solmon, F., Strahan, S., Schultz, M., Sudo, K., Szopa, S., and Wild, O.,: Nitrogen and sulfur deposition on regional and global scales: a multimodel evaluation, Global Biogeochem. Cy., 20, GB4003, doi:10.1029/2005GB002672, 2006.

Dils, B., De Mazière, M., Müller, J. F., Blumenstock, T., Buchwitz, M., de Beek, R., Demoulin, P., Duchatelet, P., Fast, H., Frankenberg, C., Gloudemans, A., Griffith, D., Jones, N., Kerzenmacher, T., Kramer, I., Mahieu, E., Mellqvist, J., Mittermeier, R. L., Notholt, J., Rinsland, C. P., Schrijver, H., Smale, D., Strandberg, A., Straume, A. G., Stremme, W., Strong, K., Sussmann, R., Taylor, J., van den Broek, M., Velazco, V., Wagner, T., Warneke, T., Wiacek, A., and Wood, S.: Comparisons between SCIAMACHY and ground-based FTIR data for total columns of CO, CH_4, CO_2 and N_2O, Atmos. Chem. Phys., 6, 1953–1976, doi:10.5194/acp-6-1953-2006, 2006.

EDGAR-Emission Database for Global Atmospheric Research: Source: EC-JRC/PBL, EDGAR version 4.2., available at: http://edgar.jrc.ec.europa.eu (last access: 15 October 2012), 2011.

Erisman, J. W., Vermetten, A. W., Asman, W. A., Waijers-Ijpelaan, A., and Slanina, J.: Vertical distribution of gases and aerosols: the behaviour of ammonia and related components in the lower atmosphere, Atmos. Environ., 22, 1153–1160, 1988.

Erisman, J. W., Otjes, R., Hensen, A., Jongejan, P., van den Bulk, P., Khlystov, A., Mols, H., and Slanina, J.: Instrument development and application in studies and monitoring of ambient ammonia, Atmos. Environ., 35, 1913–1922, 2001.

Erisman, J. W., Bleeker, A., Galloway, J., and Sutton, M. S.: Reduced nitrogen in ecology and the environment, Environ. Pollut., 150, 140–149, 2007.

Fowler, D., Coyle, M., Skiba, U., Sutton, M. A., Cape, J. N., Reis, S., Sheppard, L. J., Jenkins, A., Grizzetti, B., Galloway, J., Vitousek, P., Leach, A., Bouwman, A. F., Butterbach-Bahl, K., Dentener, F., Stevenson, D., Amann, M., and Voss, M.: The global nitrogen cycle in the twenty-first century, Philos. T. Roy. Soc. B, 368, 20130164, doi:10.1098/rstb.2013.0164, 2013.

Franco, B., Hendrick, F., Van Roozendael, M., Müller, J.-F., Stavrakou, T., Marais, E. A., Bovy, B., Bader, W., Fayt, C., Hermans, C., Lejeune, B., Pinardi, G., Servais, C., and Mahieu, E.: Retrievals of formaldehyde from ground-based FTIR and MAX-DOAS observations at the Jungfraujoch station and comparisons with GEOS-Chem and IMAGES model simulations, Atmos. Meas. Tech., 8, 1733–1756, doi:10.5194/amt-8-1733-2015, 2015.

Friedrich, R. and Reis, S. (eds.): Emissions of Air Pollutants, Springer Science and Business Media, Springer, Berlin Heidelberg New York, 2004.

Griffith, D. W. T., Jones, N. B., McNamara, B., Walsh, C. P., Bell, W., and Bernardo, C.: Intercomparison of NDSC ground-based solar FTIR measurements of atmospheric gases at Lauder, New Zealand, J. Atmos. Ocean. Tech., 20, 1138–1153, 2003.

Gyldenkærne, S., Ambelas Skjøth, C., Hertel, O., and Ellermann, T.: A dynamical ammonia emission parameterization for use in air pollution models, J. Geophys. Res.-Atmos., 110, D07108, doi:10.1029/2004JD005459, 2005.

Hansen, D. A., Edgerton, E. S., Hartsell, B. E., Jansen, J. J., Kandasamy, N., Hidy, G. M., and Blanchard, C. L.: The southeastern aerosol research and characterization study: Part 1. Overview, J. Air Waste Manage., 53, 1460–1471, doi:10.1080/10473289.2003.10466318, 2003.

Hase, F., Blumenstock, T., and Paton-Walsh, C.: Analysis of the instrumental line shape of high-resolution Fourier transform IR spectrometers with gas cell measurements and new retrieval software, Appl. Optics, 38, 3417–3422, doi:10.1364/AO.38.003417, 1999.

Hase, F., Hannigan, J. W., Coffey, M. T., Goldman, A., Höpfner, M., Jones, N. B., Rinsland, C. P., and Wood, S. W.: Intercomparison of retrieval codes used for the analysis of high-resolution, ground-based FTIR measurements, J. Quant. Spectrosc. Ra., 87, 25–52, 2004.

Hase, F., Demoulin, P., Sauval, A. J., Toon, G. C., Bernath, P. F., Goldman, A., Hannigan, J. W., Rinsland, C. P.: An empirical line-by-line model for the infrared solar transmittance spectrum from 700 to 5000 cm(−1), J. Quant. Spectrosc. Ra., 102, 450–463, doi:10.1016/j.jqsrt.2006.02.026, 2006.

Heald, C. L., Collett Jr., J. L., Lee, T., Benedict, K. B., Schwandner, F. M., Li, Y., Clarisse, L., Hurtmans, D. R., Van Damme, M., Clerbaux, C., Coheur, P.-F., Philip, S., Martin, R. V., and Pye, H. O. T.: Atmospheric ammonia and particulate inorganic nitrogen over the United States, Atmos. Chem. Phys., 12, 10295–10312, doi:10.5194/acp-12-10295-2012, 2012.

Holland, E. A., Dentener, F. J., Braswell, B. H., and Sulzman, J. M.: Contemporary and pre-industrial global reactive nitrogen budgets, Biogeochemistry, 46, 7–43, 1999.

Kerzenmacher, T., Dils, B., Kumps, N., Blumenstock, T., Clerbaux, C., Coheur, P.-F., Demoulin, P., García, O., George, M., Griffith, D. W. T., Hase, F., Hadji-Lazaro, J., Hurtmans, D., Jones, N., Mahieu, E., Notholt, J., Paton-Walsh, C., Raffalski, U., Ridder, T., Schneider, M., Servais, C., and De Mazière, M.: Validation of IASI FORLI carbon monoxide retrievals using FTIR data from NDACC, Atmos. Meas. Tech., 5, 2751–2761, doi:10.5194/amt-5-2751-2012, 2012.

Krupa, S.: Effects of atmospheric ammonia (NH_3) on terrestrial vegetation: a review, Environ. Pollut., 124, 179–221, doi:10.1016/S0269-7491(02)00434-7, 2003.

Kuenen, J., Denier van der Gon, H., Visschedijk, A., van der Brugh, H., and van Gijlswijk, R.: MACC European emission inventory for the years 2003–2007, TNO Rep. TNO-060-UT-2011-00588, TNO, Utrecht, Netherlands, 2011.

Leen, J. B., Yu, X. Y., Gupta, M., Baer, D. S., Hubbe, J. M., Kluzek, C. D., and Hubbell, M. R.: Fast in situ airborne measurement of ammonia using a mid-infrared off-axis ICOS spectrometer, Environ. Sci. Technol., 47, 10446–10453, 2013.

Lieven, C., Clerbaux, C., Dentener, F., Hurtmans, D., and Coheur, P.-F.: Global ammonia distribution derived from infrared satellite observations, Nat. Geosci., 2, 479–483, 2009.

Luo, M., Shephard, M. W., Cady-Pereira, K. E., Henze, D. K., Zhu, L., Bash, J. O., Pinder, R. W., Capps, S., and Walker, J.: Satellite observations of tropospheric ammonia and carbon monoxide: global distributions, correlations and comparisons to model simulations, Atmos. Environ., 106, 262–277, doi:10.1016/j.atmosenv.2015.02.007, 2015.

Miller, D. J., Sun, K., Tao, L., Khan, M. A., and Zondlo, M. A.: Open-path, quantum cascade-laser-based sensor for high-resolution atmospheric ammonia measurements, Atmos. Meas. Tech., 7, 81–93, doi:10.5194/amt-7-81-2014, 2014.

Mount, G. H., Rumburg, B., Havig, J., Lamb, B., Westberg, H., Yonge, D., Johnson, K, and Kincaid, R.: Measurement of atmospheric ammonia at a dairy using differential optical absorption spectroscopy in the mid-ultraviolet, Atmos. Environ., 36, 1799–1810, 2002.

Nowak, J. B., Neuman, J. A., Kozai, K., Huey, L. G., Tanner, D. J., Holloway, J. S., Ryerson, T. B., Frost, G. J., McKeen, S. A., and Fehsenfeld, F. C.: A chemical ionization mass spectrometry technique for airborne measurements of ammonia, J. Geophys. Res.-Atmos., 112, D10S02, doi:10.1029/2006JD007589, 2007.

Nowak, J. B., Neuman, J. A., Bahreini, R., Brock, C. A., Middlebrook, A. M., Wollny, A. G., Holloway, J. S., Peischl, J., Ryerson, T. B., and Fehsenfeld, F. C.: Airborne observations of ammonia and ammonium nitrate formation over Houston, Texas, J. Geophys. Res.-Atmos., 115, D22304, doi:10.1029/2010JD014195, 2010.

Paton-Walsh, C., Jones, N. B., Wilson, S. R., Haverd, V., Meier, A., Griffith, D. W., and Rinsland, C. P.: Measurements of trace gas emissions from Australian forest fires and correlations with coincident measurements of aerosol optical depth, J. Geophys. Res.-Atmos., 110, 24305, doi:10.1029/2005JD006202, 2005.

Paulot, F., Jacob, D. J., Pinder, R. W., Bash, J. O., Travis, K., and Henze, D. K.: Ammonia emissions in the United States, European Union, and China derived by high resolution inversion of ammonium wet deposition data: interpretation with a new agricultural emissions inventory (MASAGE NH_3), J. Geophys. Res.-Atmos., 119, 4343–4364, doi:10.1002/2013JD021130, 2014.

Pope III, C. A., Ezzati, M., and Dockery, D. W.: Fine-Particulate Air Pollution and Life Expectancy in the United States, New Engl. J. Med., 360, 376–386, doi:10.1056/NEJMsa0805646, 2009.

Pougatchev, N. S., Connor, B. J., and Rinsland, C. P.: Infrared measurements of the ozone vertical distribution above Kitt Peak, J. Geophys. Res.-Atmos., 100, 16689–16697, 1995.

Pouliot, G., Pierce, T., van der Gon, H. D., Schaap, M., Moran, M., and Nopmongcol, U.: Comparing emission inventories and model-ready emission datasets between Europe and North America for the AQMEII project, Atmos. Environ., 53, 4–14, doi:10.1016/j.atmosenv.2011.12.041, 2012.

Puchalski, M. A., Sather, M. E., Walker, J. T., Lehmann, C. M., Gay, D. A., Mathew, J., and Robarge, W. P.: Passive ammonia monitoring in the United States: comparing three different sampling devices, J. Environ. Monit., 13, 3156–3167, doi:10.1039/c1em10553a, 2011.

Rao, K. N. and Weber, A.: Spectroscopy of the Earth's Atmosphere and Interstellar Medium, Academic, San Diego, CA, 1992

Reay, D. S., Dentener, F., Smith, P., Grace, J., and Feely, R. A.: Global nitrogen deposition and carbon sinks, Nat. Geosci., 1, 430–437, 2008.

Rodgers, C. D.: Inverse Methods for Atmospheric Sounding: Theory and Practice, vol. 2, World Scientific, Singapore, 2000.

Rodhe, H., Dentener, F., and Schulz, M.: The global distribution of acidifying wet deposition, Environ. Sci. Technol., 36, 4382–4388, 2002.

Rothman, L. S., Gordon, I. E., Babikov, Y., Barbe, A., Chris Benner, D., Bernath, P. F., Birk, M., Bizzocchi, L., Boudon, V., Brown, L. R., Campargue, A., Chance, K., Cohen, E. A., Coudert, L. H., Devi, V. M., Drouin, B. J., Fayt, A., Flaud, J.-M., Gamache, R. R., Harrison, J. J., Hartmann, J.-M., Hill, C., Hodges, J. T., Jacquemart, D., Jolly, A., Lamouroux, J., Le Roy, R. J., Li, G., Long, D. A., Lyulin, O. M., Mackie, C. J., Massie, S. T., Mikhailenko, S., Müller, H. S. P., Naumenko, O. V., Nikitin, A. V., Orphal, J., Perevalov, V., Perrin, A., Polovtseva, E. R., Richard, C., Smith, M. A. H., Starikova, E., Sung, K., Tashkun, S., Tennyson, J., Toon, G. C., Tyuterev, G., and Wagner, G.: The HITRAN2012 molecular spectroscopic database, J. Quant. Spectrosc. Ra., 130, 4–50, 2013.

Rodgers, C. D. and Connor, B. J.: Intercomparison of remote sounding instruments, J. Geophys. Res.-Atmos., 108, 4116–4229, 2003.

Schaap, M., van Loon, M., ten Brink, H. M., Dentener, F. J., and Builtjes, P. J. H.: Secondary inorganic aerosol simulations for Europe with special attention to nitrate, Atmos. Chem. Phys., 4, 857–874, doi:10.5194/acp-4-857-2004, 2004.

Shephard, M. W., Cady-Pereira, K. E., Luo, M., Henze, D. K., Pinder, R. W., Walker, J. T., Rinsland, C. P., Bash, J. O., Zhu, L., Payne, V. H., and Clarisse, L.: TES ammonia retrieval strategy and global observations of the spatial and seasonal variability of ammonia, Atmos. Chem. Phys., 11, 10743–10763, doi:10.5194/acp-11-10743-2011, 2011.

Shephard, M. W. and Cady-Pereira, K. E.: Cross-track Infrared Sounder (CrIS) satellite observations of tropospheric ammonia, Atmos. Meas. Tech., 8, 1323–1336, doi:10.5194/amt-8-1323-2015, 2015.

Skjøth, C. A., Geels, C., Berge, H., Gyldenkærne, S., Fagerli, H., Ellermann, T., Frohn, L. M., Christensen, J., Hansen, K. M., Hansen, K., and Hertel, O.: Spatial and temporal variations in ammonia emissions – a freely accessible model code for Europe, Atmos. Chem. Phys., 11, 5221–5236, doi:10.5194/acp-11-5221-2011, 2011.

Sussmann, R., Borsdorff, T., Rettinger, M., Camy-Peyret, C., Demoulin, P., Duchatelet, P., Mahieu, E., and Servais, C.: Technical Note: Harmonized retrieval of column-integrated atmospheric water vapor from the FTIR network – first examples for long-term records and station trends, Atmos. Chem. Phys., 9, 8987–8999, doi:10.5194/acp-9-8987-2009, 2009.

Sutton, M. A., Reis, S., Riddick, S., Dragosits, U., Nemitz, E., Theobald, M. R., Tang, S., Braban, C. F., Vieno, M., Dore, A. J., Mitchell, R. F., Wanless, S., Daunt, F., Fowler, D., Blackall, T., Milford, C., Flechard, C., Loubet, B., Massad, R. S., Cellier, P., Clarisse, L., van Damme, M., Ngadi, N., Clerbaux, C., Skjøth, C., Geels, C., Hertel, O., Wichink Kruit, R. J., Pinder, R. W., Bash, J. O., Walker, J. D., Simpson, D., Horvath, L., Misselbrook, T., Bleeker, A., Dentener, F., and de Vries, W.: Towards a climate-dependent paradigm of ammonia emission and deposition, Philos. T. Roy. Soc. B, 368, 20130166, doi:10.1098/rstb.2013.0166, 2013.

Thijsse, T. R., Duyzer, J. H., Verhagen, H. L. M., Wyers, G. P., Wayers, A., and Möls, J. J.: Measurement of ambient ammonia with diffusion tube samplers, Atmos. Environ., 32, 333–337, 1998.

Thomas, R. M., Trebs, I., Otjes, R., Jongejan, P. A. C., ten Brink, H., Phillips, G., Kortner, M., Meixner, F. X., and Nemitz, E.: An automated analyzer to measure surface–atmosphere exchange fluxes of water soluble inorganic aerosol compounds and reactive trace gases, Environ. Sci. Technol., 43, 1412–1418, 2009.

Toon, G. C., Blavier, J.-F., Sen, B., Margitan, J. J., Webster, C. R., Max, R. D., Fahey, D. W., Gao, R., DelNegro, L., Proffitt, M., Elkins, J., Romashkin, P. A., Hurst, D. F., Oltmans, S., Atlas, E., Schauffler, S., Flocke, F., Bui, T. P., Stimpfle, R. M., Bonne, G. P., Voss, P. B., and Cohen, R. C.: Comparison of MkIV balloon and ER-2 aircraft measurements of atmospheric trace gases, J. Geophys. Res., 104, 26779–26790, 1999.

Van Damme, M., Clarisse, L., Heald, C. L., Hurtmans, D., Ngadi, Y., Clerbaux, C., Dolman, A. J., Erisman, J. W., and Coheur, P. F.: Global distributions, time series and error characterization of atmospheric ammonia (NH_3) from IASI satellite observations, Atmos. Chem. Phys., 14, 2905–2922, doi:10.5194/acp-14-2905-2014, 2014a.

Van Damme, M., Wichink Kruit, R. J., Schaap, M., Clarisse, L., Clerbaux, C., Coheur, P.-F., Dammers, E., Dolman, A. J., and Erisman, J. W.: Evaluating 4 years of atmospheric ammonia (NH_3) over Europe using IASI satellite observations and LOTOS-EUROS model results, J. Geophys. Res. Atmos., 119, 9549–9566, doi:10.1002/2014JD021911, 2014b.

Van Damme, M., Clarisse, L., Dammers, E., Liu, X., Nowak, J. B., Clerbaux, C., Flechard, C. R., Galy-Lacaux, C., Xu, W., Neuman, J. A., Tang, Y. S., Sutton, M. A., Erisman, J. W., and Coheur, P. F.: Towards validation of ammonia (NH_3) measurements from the IASI satellite, Atmos. Meas. Tech., 8, 1575–1591, doi:10.5194/amt-8-1575-2015, 2015a.

Van Damme, M., Erisman, J. W., Clarisse, L., Dammers, E., Whitburn, S., Clerbaux, C., Dolman, A. J., and Coheur, P. F.: Worldwide spatiotemporal atmospheric ammonia (NH_3) variability revealed by satellite, Geophys. Res. Lett., in revision, 2015b.

Van Putten, E. M., Mennen, M. G., Regts, T., and Uiterwijk, J. W.: Performance Study of Four Automatic Ammonia Monitors Under Controlled Conditions, report 723101004, RIVM, Bilthoven, 1994.

Vigouroux, C., Stavrakou, T., Whaley, C., Dils, B., Duflot, V., Hermans, C., Kumps, N., Metzger, J.-M., Scolas, F., Vanhaelewyn, G., Müller, J.-F., Jones, D. B. A., Li, Q., and De Mazière, M.: FTIR time-series of biomass burning products (HCN, C_2H_6, C_2H_2, CH_3OH, and

HCOOH) at Reunion Island (21° S, 55° E) and comparisons with model data, Atmos. Chem. Phys., 12, 10367–10385, doi:10.5194/acp-12-10367-2012, 2012.

Vigouroux, C.: EGU, Ground-based FTIR Measurements of NH_3 Total Columns and Comparison with IASI Data, Vienna, Austria, id. EGU2013-11785, 2013.

Vitousek, P. M., Aber, J., Howarth, R. W., Likens, G. E., Matson, P. A., Schindler, D. W., Schlesinger, W. H., and Tilman, G. D.: Human Alteration of the Global Nitrogen Cycle: Causes and Consequences, Ecological Society of America, Washington, DC, US, 1997.

Volten, H., Bergwerff, J. B., Haaima, M., Lolkema, D. E., Berkhout, A. J. C., van der Hoff, G. R., Potma, C. J. M., Wichink Kruit, R. J., van Pul, W. A. J., and Swart, D. P. J.: Two instruments based on differential optical absorption spectroscopy (DOAS) to measure accurate ammonia concentrations in the atmosphere, Atmos. Meas. Tech., 5, 413–427, doi:10.5194/amt-5-413-2012, 2012.

von Bobrutzki, K., Braban, C. F., Famulari, D., Jones, S. K., Blackall, T., Smith, T. E. L., Blom, M., Coe, H., Gallagher, M., Ghalaieny, M., McGillen, M. R., Percival, C. J., Whitehead, J. D., Ellis, R., Murphy, J., Mohacsi, A., Pogany, A., Junninen, H., Rantanen, S., Sutton, M. A., and Nemitz, E.: Field inter-comparison of eleven atmospheric ammonia measurement techniques, Atmos. Meas. Tech., 3, 91–112, doi:10.5194/amt-3-91-2010, 2010.

Whitburn, S., Van Damme, M., Kaiser, J. W., van der Werf, G. R., Turquety, S., Hurtmans, D., Clarisse, L., Clerbaux, C., and Coheur, P. F.: Ammonia emissions in tropical biomass burning regions: comparison between satellitederived emissions and bottom-up fire inventories, Atmos. Environ., doi:10.1016/j.atmosenv.2015.03.015, in press, 2015.

Zander, R., Mahieu, E., Demoulin, P., Duchatelet, P., Roland, G., Servais, C., De Mazière, M., Reimann, S., and Rinsland, C. P.: Our changing atmosphere: evidence based on long-term infrared solar observations at the Jungfraujoch since 1950, Sci. Total Environ., 391, 184–195, 2008.

Table 1. FTIR stations used in the analysis. The location, longitude, latitude and altitude are given for each station as well as the instrument used for the measurements. Some station specifics are given in the last column.

Station	Location	Longitude	Latitude	Altitude (m a.s.l.)	Instrument	Station specifics
Bremen	Germany	8.85° E	53.10° N	27	Bruker 125 HR	City, fertilizers, livestock
Lauder	New Zealand	169.68° E	45.04° S	370	Bruker 120 HR	Fertilizers, livestock
Reunion	Indian Ocean	55.5° E	20.90° S	85	Bruker 120M	Fertilizers, fires
Jungfraujoch	Switzerland	7.98° E	46.55° N	3580	Bruker 120 HR	High altitude, no large sources

Table 2. Micro windows used in the NH_3 retrieval at the four stations.

Stations	Micro window	Spectral range (cm^{-1})	Interfering species (Profile retrieved species in **bold**)	SNR
Bremen and Lauder	MW1	930.32–931.32	**NH_3**, **H_2O**, **O_3**, CO_2, N_2O, HNO_3, SF_6, CFC-12, solar lines	Bremen – Real SNR mean value of 450
	MW2	966.97–967.68	**NH_3**, **H_2O**, **O_3**, CO_2, N_2O, HNO_3, solar lines	Lauder – Real SNR mean value of 250
Reunion	MW1	929.4–931.4	**NH_3**, **H_2O**, O_3, CO_2, N_2O, HNO_3, SF_6, CFC-12	Reunion – Real SNR mean value of 365
	MW2	962.1–970.0	**NH_3**, **H_2O**, O_3, CO_2, N_2O, HNO_3, HDO, $^{686}O_3$, solar lines	
Jungfraujoch	MW1	929.4–931.4	**NH_3**, H_2O, O_3, CO_2, N_2O, HNO_3, SF_6, CFC-12	
	MW2	962.1–970.0	**NH_3**, H_2O, O_3, CO_2, N_2O, HDO, $^{686}O_3$, solar lines	**Jungfraujoch – Fixed at 250**

Table 3. Random and Systematic uncertainties used in the error calculation.

Version (Stations)	SFIT 4 (Bremen, Lauder, Reunion)		Version (Stations)	SFIT 2 (Jungfraujoch)	
Parameter	Random uncertainty	Systematic uncertainty	Parameter	Random uncertainty	Systematic uncertainty
Temperature	2 K troposphere 5 K stratosphere	2 K troposphere 5 K stratosphere	Temperature	1.5 K 0–20 km 2.0 K 20–30 km 5.0 K 30 km–	
Solar line shift	0.005 cm^{-1}	0.005 cm^{-1}	Line intensity		20.0 %
Solar line strength	0.1 %	0.1 %	Line T broadening		10.0 %
Solar zenith angle	0.01°	0.01°	Line P broadening		10.0 %
Phase	0.001 Rad	0.001 Rad	Interfering species		HITRAN2012: varies
Zero level	0.01	0.01	Instrumental Line Shape (ILS)		10 %
Background curvature		0.001 cm^{-2}	Influence a priori profiles	Calculated	
Field of view		0.001	Solar Zenith Angle (SZA)	0.2°	
Line intensity		20.0 %			
Line T broadening		10.0 %			
Line P broadening		10.0 %			
Interfering species	HITRAN2012: varies				

Table 4. Mean random and systematic errors for each of the individual NH_3 retrieval parameters. The table is split into two sections to cover both the error calculation using SFIT4 (Bremen, Lauder, Reunion) and SFIT2 (Jungfraujoch). At the bottom the errors are summarized into total mean errors for each of the stations.

Station	Bremen		Lauder		Reunion			Jungfraujoch	
Parameter	Mean Random Error (%)	Mean Systematic Error (%)	Mean Random Error (%)	Mean Systematic Error (%)	Mean Random Error (%)	Mean Systematic Error (%)	Parameter	Mean Random Error (%)	Mean Systematic Error (%)
Temperature	4.9	4.9	3.6	3.6	2.7	2.9	Temperature	15.2	
Solar zenith angle	1.6	1.6					Solar zenith angle	1.9	
Phase	1.0	1.0	1.1	1.1			Instrumental lineshape		1.4
Zero level	5.0	5.0	6.8	6.8					
Measurement noise	4.5		8.4		10.9		Measurement noise	18.2	
Interfering Species	1.3		2.4		0.9	8.7 (H_2O line pressure broadening)	Interfering species		1.4
Retrieval parameters	0.1		0.1				Model parameters	1.4	
Background curvature		1.1		1.2		0.3	Forward model		1.0
Smoothing error		2.8		8.1	10.3		Smoothing	5.4	
Spectroscopy		21.0		22.7		17.8	Spectroscopy		20.1
							NH_3 a priori		6.1
							Influence a priori profiles (H_2O and HDO)	6.6	
Subtotal error	9.1	23.5	12.0	27.0	15.3	20.0	Subtotal error	25.3	23.1
Total error	25.8		30.2		25.2		Total	34.2	

Table 5. Statistics of the NH_3 columns. (Nr: number of data points, DOFS: Degree of Freedom for Signal, Mean ± the error of the mean, RMS: Root Mean Square). Total columns are given in 1×10^{15} molecules $NH_3\,cm^{-2}$.

Station	Nr	Mean DOFS	Mean (molecules × 1 × 10^{15})	Median (molecules × 1 × 10^{15})	RMS (molecules × 1 × 10^{15})
Bremen	554	1.9	13.75 ± 4.24	9.51	20.22
Lauder	2412	1.4	4.17 ± 1.40	2.85	5.95
Reunion	1262	1.0	0.80 ± 0.54	0.56	1.14
Jungfraujoch	2702	1.0	0.18 ± 0.07	0.15	0.22

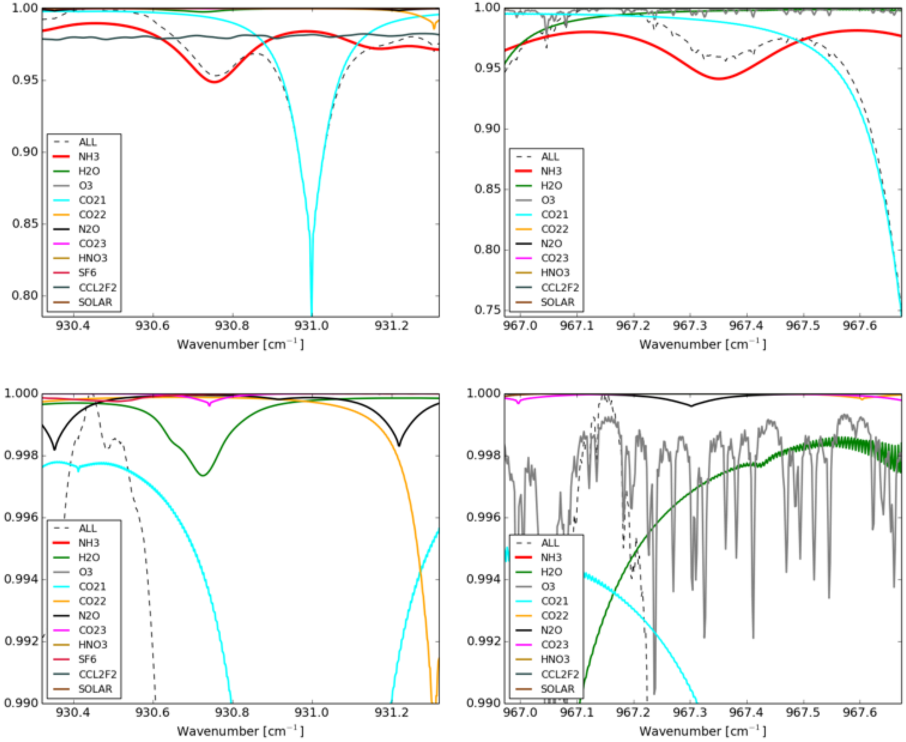

Figure 1. Calculated spectrum for both spectral windows measured with the 125HR in Bremen on the 19 April 2010 at 09:59 (UTC) corresponding to a total column of 18.83×10^{15} molecules cm^{-2}. The top two panels show the individual contributions of the different species in the first (MW1) and second (MW2) spectral windows. The second row show the same calculated spectra but now with the *y* axis scaled to show the minor interfering species.

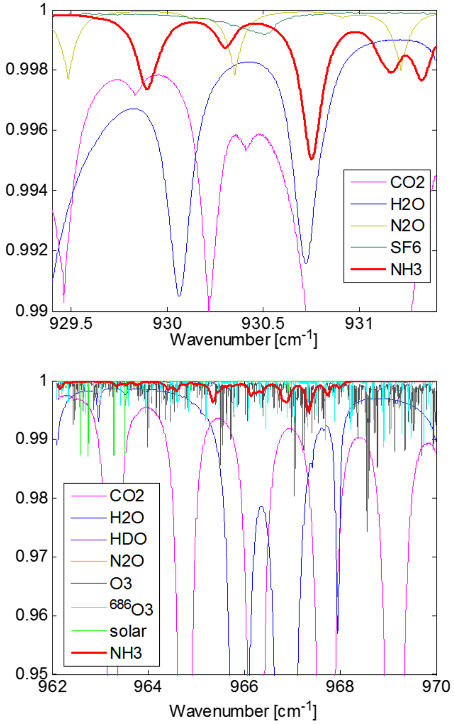

Figure 2. Example of a synthetic atmospheric spectrum for both spectral windows at Reunion Island, computed for the 5 June 2011 and a total column of 1.07×10^{15} molecules cm^{-2}. The top panel shows the individual contributions of the main species in the first spectral window. The bottom panel shows the second spectral window.

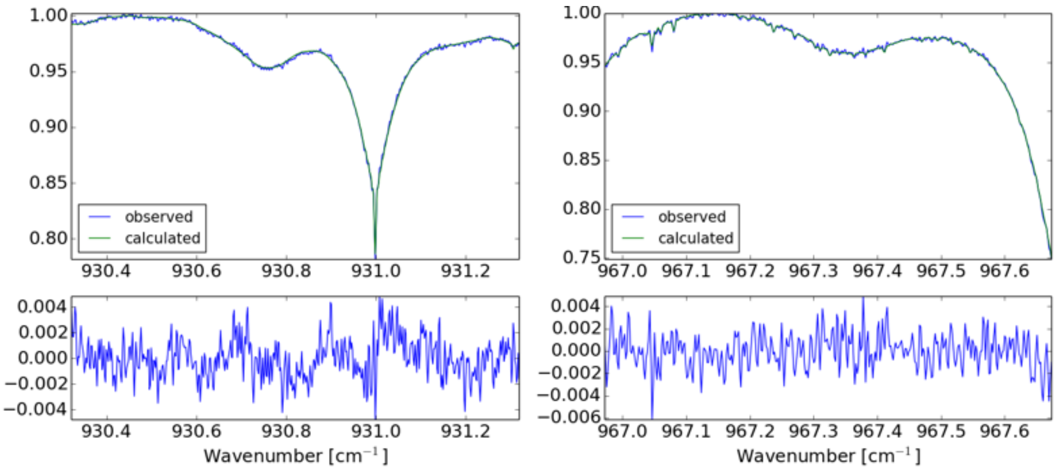

Figure 3. Measured and calculated spectrum for both spectral windows measured with the 125HR in Bremen on the 19 April 2010 at 09:59 (UTC) corresponding to a total column of 18.83×10^{15} molecules NH_3 cm^{-2}. The top two panels show the observed (blue line) and calculated (green line) spectra for MW1 (left) and MW2 (right). The bottom two figures show the residuals of the fits in both spectral windows.

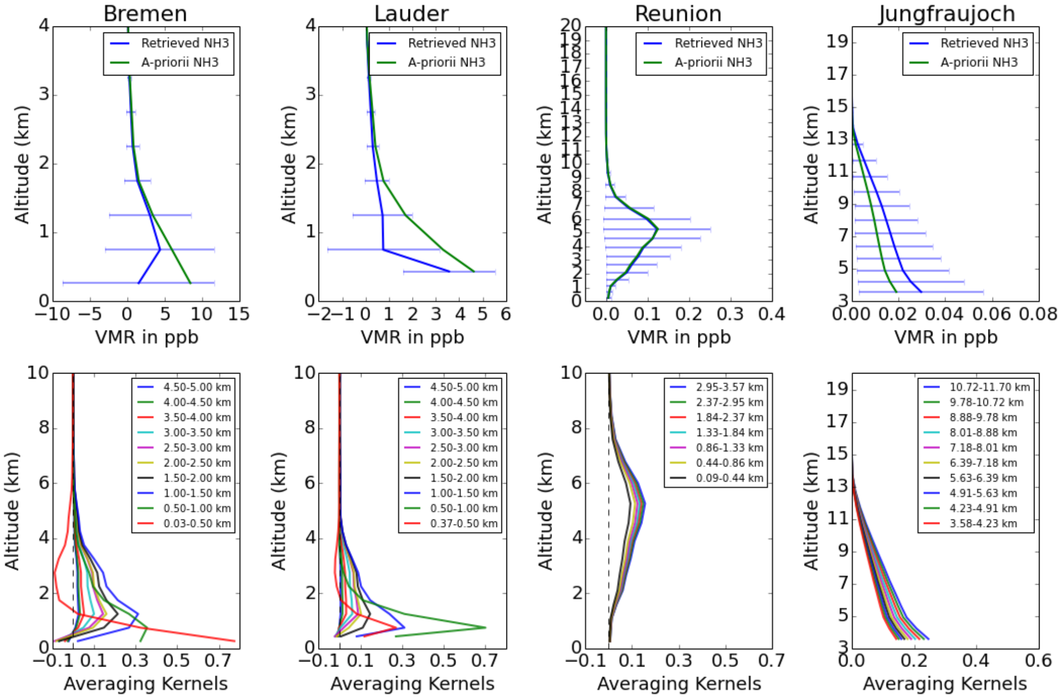

Figure 4. Top panels: the retrieved NH_3 profile (blue) and the a-priori profile (green) in order from left to right: Bremen (Left), Lauder (Left middle), Reunion island (right middle) and Jungfraujoch (right). Horizontal lines indicate the standard deviation in all observations for each layer. Bottom panels: the normalized averaging kernel for each of the stations.

Title Page
Abstract
Introduction
Conclusions
References
Tables
Figures
◀▮
▶▮
◀
▶
Back
Close
Full Screen / Esc
Printer-friendly Version
Interactive Discussion

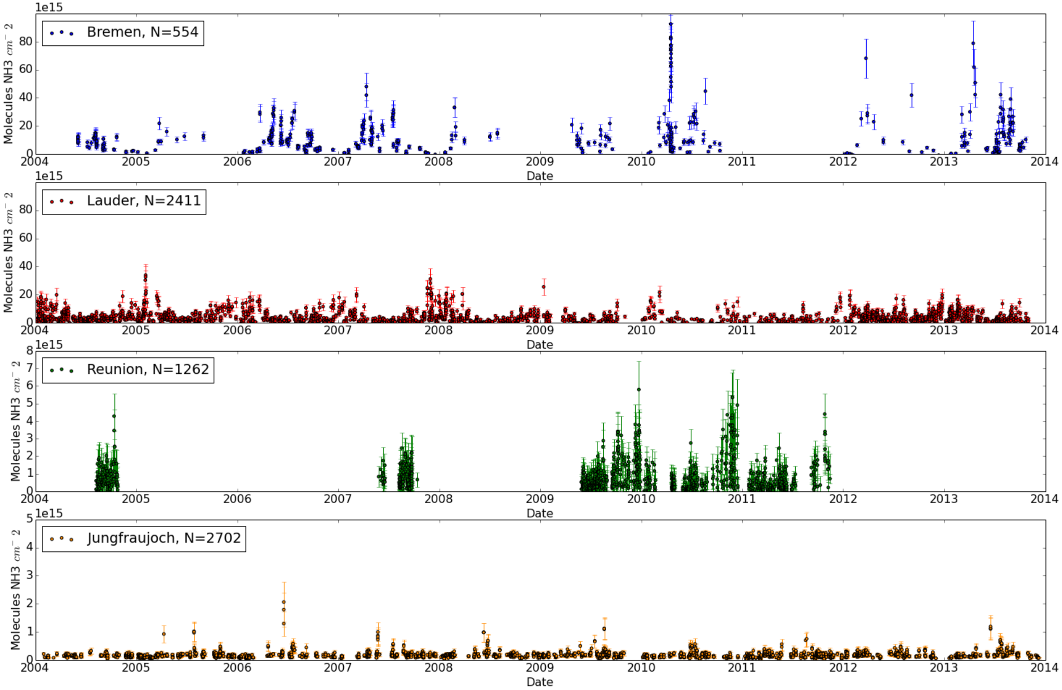

Figure 5. Time series of retrieved NH_3 columns (in molecules $NH_3\,cm^{-2}$). From top to bottom the figure shows the Bremen (blue), Lauder (red), Reunion (green) and Jungfraujoch (yellow) total columns. The bars reflect the errors on the individual observations.

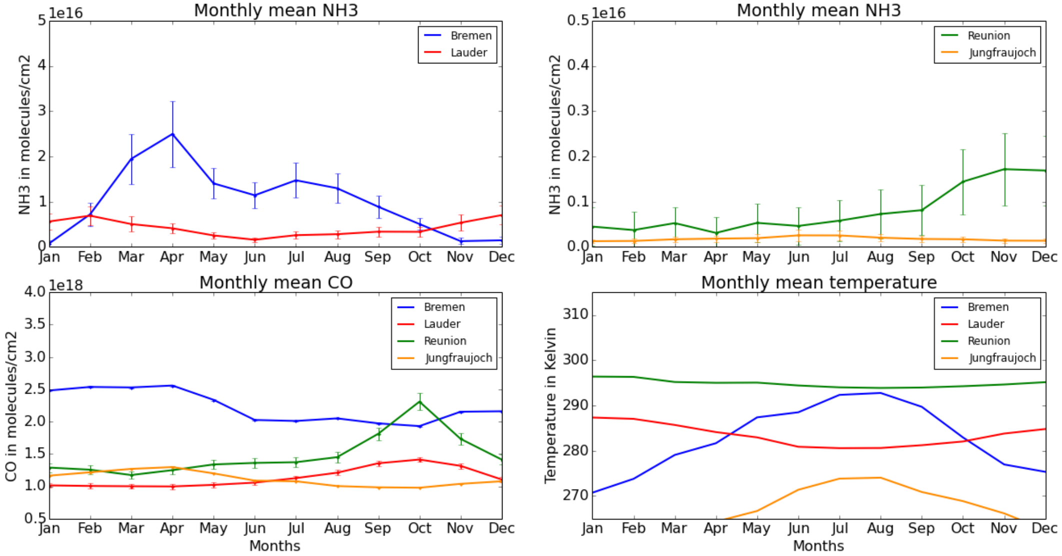

Figure 6. 2004–2013 monthly averaged columns for NH_3, CO and temperature. The top two panels show the monthly NH_3 column concentrations (molecules $NH_3\,cm^{-2}$) for each of the four stations. Vertical lines indicate the mean monthly error. The bottom two panels show additional column concentrations of CO (bottom, left) and temperature (bottom, right).

Title Page
Abstract
Introduction
Conclusions
References
Tables
Figures
◀◀
▶▶
◀
▶
Back
Close
Full Screen / Esc
Printer-friendly Version
Interactive Discussion